LBL-30075
Preprint

Lawrence Berkeley Laboratory
UNIVERSITY OF CALIFORNIA

Materials & Chemical Sciences Division

To be published as a chapter in **Recent Progress in the Study of Vacuum Ultraviolet Ionization and Dissociation of Molecules and Clusters**, C.Y. Ng, Ed., World Scientific, Singapore, Republic of Singapore, 1991

Spectroscopy and Reaction Dynamics Using Ultrahigh Resolution VUV Lasers

A.H. Kung and Y.T. Lee

December 1990

LOAN COPY
Circulates
for 2 weeks
Bldg. 50 Library.
LBL-30075
Copy 2

Prepared for the U.S. Department of Energy under Contract Number DE-AC03-76SF00098

DISCLAIMER

This document was prepared as an account of work sponsored by the United States Government. While this document is believed to contain correct information, neither the United States Government nor any agency thereof, nor the Regents of the University of California, nor any of their employees, makes any warranty, express or implied, or assumes any legal responsibility for the accuracy, completeness, or usefulness of any information, apparatus, product, or process disclosed, or represents that its use would not infringe privately owned rights. Reference herein to any specific commercial product, process, or service by its trade name, trademark, manufacturer, or otherwise, does not necessarily constitute or imply its endorsement, recommendation, or favoring by the United States Government or any agency thereof, or the Regents of the University of California. The views and opinions of authors expressed herein do not necessarily state or reflect those of the United States Government or any agency thereof or the Regents of the University of California.

LBL-30075

SPECTROSCOPY AND REACTION DYNAMICS USING ULTRAHIGH RESOLUTION VUV LASERS

A. H. Kung and Yuan T. Lee

Department of Chemistry
University of California

and

Chemical Sciences Division
Lawrence Berkeley Laboratory
Berkeley, CA 94720 USA

December 1990

This work was supported by the Director, Office of Energy Research, Office of Basic Energy Sciences, Chemical Sciences Division, of the U.S. Department of Energy under Contract No. DE-AC03-76SF00098.

Studies in single-collision and isolated-molecule conditions allow the elucidation of microscopic molecular behavior.

The most productive means in carrying out chemical dynamics studies on small systems is detailed characterization of the nature of the transition state region of a reaction and the state of reaction products, i.e., state-to-state population distribution, translational energy distribution, and preferred orientations of angular momenta of the products. This characterization requires completely mapping out the quantum-state distribution, and the velocity and angular distribution of the products. High resolution photofragmentation-translational spectroscopy has been highly successful in elucidating the dynamics of dissociation processes by determining velocity and angle-resolved distributions of products.[1] However, the method, except for some very favorable cases, does not have sufficient resolution to provide detailed information on product quantum-state distribution. There are many approaches to accomplish state-resolved detection. Laser induced fluorescence (LIF), multiphoton ionization (MPI), infrared absorption, and coherent Raman scattering are the more commonly used methods. These methods have high sensitivity and have been successful in several selected cases where the known fragments are atoms or small diatomic molecules which have transitions of known strengths and wavelengths that are accessible to available tunable sources.

Successful reaction dynamics studies often hinges on having a good knowledge of the spectroscopy of the fragments produced in a reaction. While each individual reaction may have its own optimal method of study, it is highly desirable to have one approach that is generally applicable to many reactions of interest. The technique of resonance-enhanced multiple-photon ionization (REMPI) appears to be the desirable approach. It has been widely used as a spectroscopic tool and for gas phase detection of atoms and molecules.[2] There are many advantages of REMPI over techniques like LIF, Raman, and direct absorption: it is applicable to most molecular fragments that have accessible electronic resonances; it is highly sensitive because the detection of ions can be 100%; it is specie specific and state specific because it utilizes state-specific resonance excitation of the radical or molecule; when used in conjunction with either a time-of-flight or a quadrupole mass spectrometer the method is often practically background free. The disadvantage of REMPI, however, is that it is a non-linear process that requires use of high power pulsed lasers and often involves dipole-forbidden transitions. While this does not affect the accuracy in determining line positions it makes quantitative state-resolved population analysis difficult using the ion signal measurements.

The specific case of one-photon-resonant excitation followed by one-photon ionization (1+1 REMPI, figure 1) is an exception to this. With a weak, high-resolution photon being tuned on to resonance and to remain below saturation level, and an intense second photon used to induce ionization, the ion signal will be *linearly* proportional to the single photon absorption cross-section of the initial quantum state. These conditions can be easily achieved in real experimental situations and has been demonstrated in an experiment using room temperature H_2.[3] The one-to-one mapping of ion signals to the absorption cross-section can be made easily by taking accurately known Franck-Condon factors into account. This makes high-resolution (1+1) REMPI a very powerful technique to extract quantitative

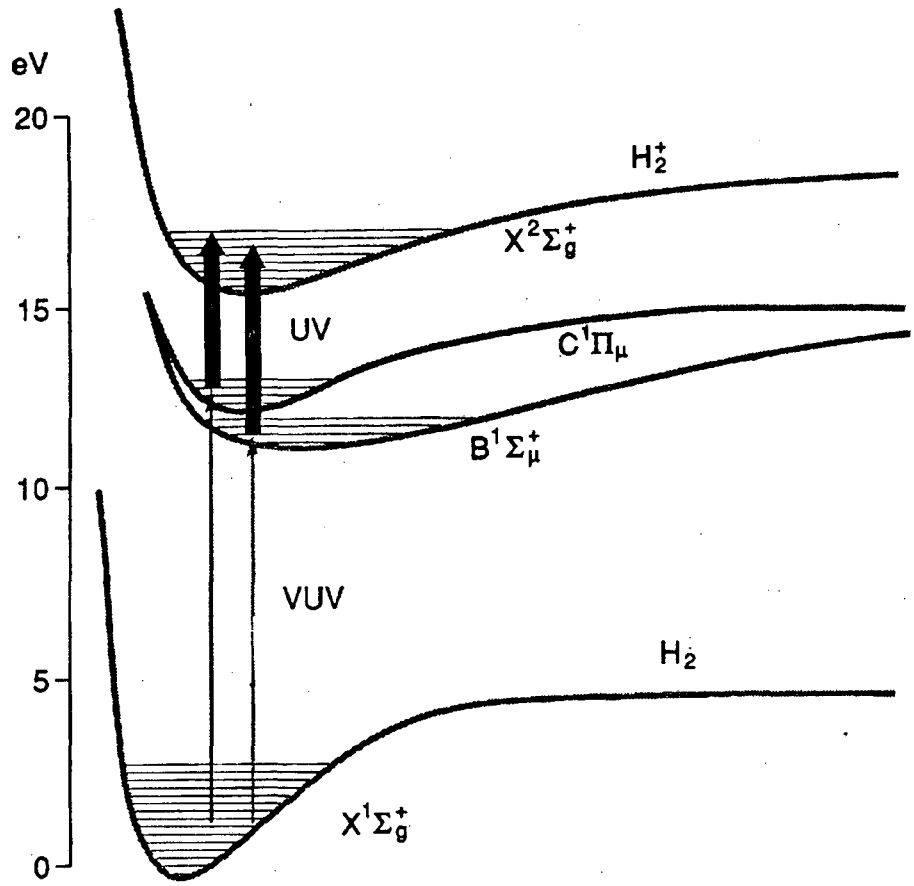

Figure 1. The (1+1) REMPI process is illustrated using the H_2 potential energy diagram. The H_2 molecule is excited by a weak VUV photon. A second intense UV photon is then used to ionize the excited molecule.

spectroscopic information of atoms and molecules. With high-resolution VUV or XUV excitation as the first step, (1+1) photon ionization becomes possible even for those molecules with high electronic excitation energies. The ionizing photon typically is in the UV or visible. If the ionizing photon is from a source independent of the source which is used to generate the VUV photon by tripling or frequency mixing techniques, its intensity can be set to suppress higher order REMPI processes. Furthermore, if the second source is tunable, its wavelength can be chosen for best selectivity, e.g., to avoid excitation of autoionization resonances which may change the ionic state distribution. Of course, the versatile (1+1) REMPI technique is also a very powerful tool for studying high-resolution spectroscopy. Tunable VUV absorption plus UV ionization permits the extraction of detailed spectroscopic information on excited electronic states and Rydberg states of many atoms, polyatomic molecules and free radicals. These spectroscopic information are needed to apply (1+1) REMPI to dynamics studies. Tunable IR absorption plus VUV ionization, alternatively, provides details of ro-vibrational states and hence the

structure of these species. If a fixed first photon is used to excite a molecule to a certain level and a tunable second photon to ionize either through autoionization or direct ionization, then spectroscopy of symmetry forbidden transitions or ionic states can be obtained.

A very-high-resolution laser source is essential for proper execution of many of these applications. For example, the Doppler profiles of photodissociation H_2 products with an energy spread of 20 kcal/mole are typically a few wavenumbers wide in the VUV. To observe details of the Doppler profile for the determination of velocity distribution, a source with resolution much better than 0.1 cm^{-1} in the visible will be required. High-resolution VUV lasers have been widely applied in many laboratories in a variety of spectroscopic and reaction dynamics studies.[4-7] In the next section we describe the construction of a ultra-high-resolution VUV source used in our laboratory in several experiments that exploit the (1+1) REMPI technique. Results of these experiments are described in the subsequent sections.

II. Ultrahigh Resolution VUV Laser Source

In order to fully utilize VUV+UV REMPI, it is necessary to have the best possible VUV laser source for the first step of excitation. Transform-limited tunable lasers with a pulse duration of several nanocesonds which represent photon sources with the highest spectral purity and spectral brightness are certainly the best choice. Near transform-limited tunable nanosecond lasers have long been available but their operation has been limited to the visible and UV region.[8] It is clearly desirable to extend the wavelength coverage to the VUV and XUV. We shall describe here the basic requirements and the approach that was taken to construct a ultrahigh resolution VUV source for photoionization and LIF study of small to intermediate sized molecules in a pulsed molecular beam setting.

The first and foremost requirement is that the source be continuously tunable over the range of 70 nm to 160 nm. Other important requirements include high spectral brightness, transform-limited spectral resolution, and high intensity in the range of 10^{16} to 10^{17} photons per cm^2 per second. Many experiments will also benefit from having an illuminated spot with a uniform spatial profile and from having a user friendly source.

Although there are many approaches to produce VUV laser light, the tunability requirement predicated the use of the technique of four-wave mixing and its degenerate case of third harmonic generation. This well-established technique has very broad wavelength coverage and allows substantial use of reliable commercial components. In our laboratory the following were chosen to constitute the major components of our VUV source:

* a pulse-amplified CW single-longitudinal-mode dye laser for good frequency control;
* an injection-seeded Nd:YAG laser as pump laser for a smooth Gaussian temporal profile;
* side-pumped prism dye cells to preserve the spatial quality of the dye beam;

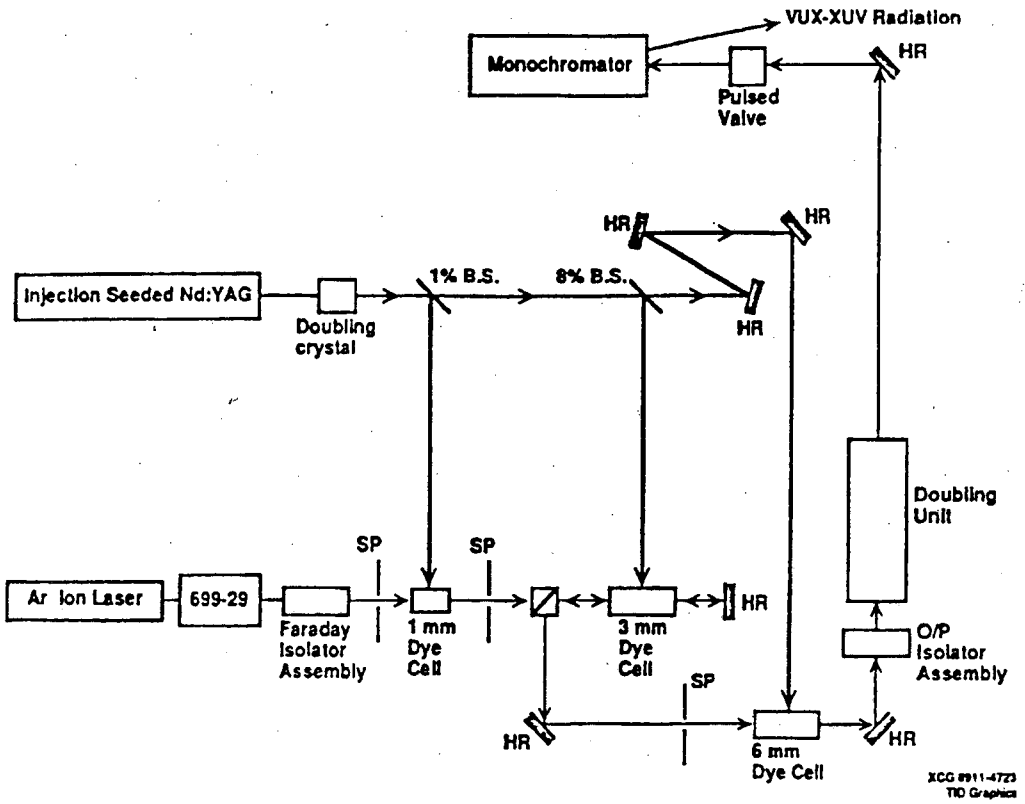

Figure 2. Schematic of one leg of the ultrahigh resolution laser system. (BS = beamsplitter, HR = high reflecting mirror, and SP = spatial filter/telescope). Reprinted with permission from Reference 9.

* a pulsed nozzle as the VUV generator for simplicity and flexibility in the choice of four-wave mixing medium;
* a 1-meter grating monochromator to disperse the VUV-XUV wavelengths from the incident visible and UV radiation.
* a Faraday optical rotator for isolation of the CW dye laser from the pulsed dye amplifiers;
* lens-pinhole-lens spatial filtering between successive stages of dye amplification to control amplified-spontaneous-emission growth.

Auto-tracked second-harmonic-generation crystals convert the visible to the UV prior to the four-wave mixing stage. Figure 2 shows the layout of the high-resolution VUV laser system. This system provides one transform-limited beam of visible and UV radiation for the four-wave mixing process. A second, identical setup provides the second beam. The wavelengths used in the mixing process span a broad range in the visible and the UV. Hence, a UV achromat is installed to give good spatial overlap of the beams at the focal point of the lens underneath the exit of a pulsed where the VUV is generated. At least a factor of five increase in VUV power was observed in non-resonant mixing when the achromat was installed. Table I is a summary of the performance of the laser. Entries to the table are self-explanatory. It is however necessary to point out that we measured a frequency shift of 0 to ~20 MHz between the CW laser frequency and the amplified output frequency. This shift depends on

the dye used as well as the number of amplification stages used. For experiments where this shift can affect the accuracy of the results it is necessary to determine the shift for each frequency measurement. For the reader who is interested in a detail description of the characterization of the laser, the information is provided in reference 9.

Table I: Summary of Laser Performance

	Visible	UV	VUV-XUV
Energy	100 mJ	30 mJ	1 μJ
Bandwidth (FWHM)	91 MHz	140 MHz	210 MHz
Pulsewidth	7 nsec	< 7 nsec	≤ 4 nsec
Temporal Profile	near Gaussian	near Gaussian	near Gaussian
Tuning Range (tested)	562-680 nm	281-340 nm 210-240 nm	74-124 nm
Frequency Shift	Amplifier configuration and dye dependent		

III. Ultrahigh-resolution Spectroscopy

The first application of our VUV laser described in the previous section is to determine the hyperfine structures, isotope shifts and lifetimes for the lower Rydberg levels of krypton.[10] The experiment demonstrates a case in (1+1) REMPI where the first photon probes spectroscopic information of energy levels while the second photon serves as a detector of that information.

There is an urgent need for high resolution VUV data in atomic and molecular spectroscopy. Many important physical and chemical processes, such as separation of rare isotopes and dating of prehistoric samples, become relatively simple if the highly selective and sensitive (1+1) REMPI technique can be utilized. However, precise knowledge of electronic transitions of most atoms and simple molecules that are needed for (1+1) REMPI has not been studied in detail as they fall in the VUV and XUV region of the spectrum. An excellent benchmark example to demonstrate the need for ultrahigh resolution spectroscopy in the VUV is krypton. The 605.78 nm line of ^{86}Kr was chosen as the primary wavelength standard. Transitions between excited states, starting mostly from metastable Kr, have been measured with very

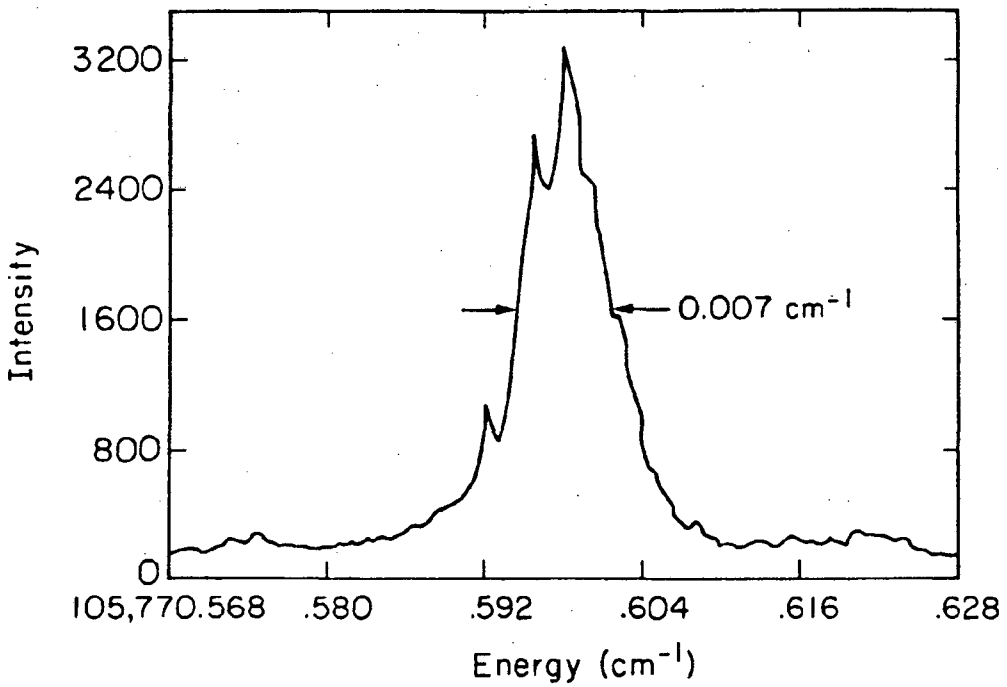

Figure 3. Scan of the 4p-7s $^2P_{3/2}$ (J = 1) transition of Kr at 94.5 nm. FWHM = 210 MHz (0.007 cm^{-1}). Reprinted with permission from Reference 9.

high accuracy. However, the absolute frequency of the Kr transitions relative to the ground state is known only to within ± 0.15 cm^{-1}. In addition, out of six stable isotopes of mass 78, 80, 82, 83, 84 and 86, only ^{83}Kr has a non-zero nuclear angular momentum, but the hyperfine splittings for ground state transitions have not been determined. There is also evidence of irregularities in the degree of contribution of the nuclear volume to the isotope shifts of Kr.[11,12] Precise high resolution spectroscopy from the ground state will shed some light in this regard.

Using a pulsed beam of Kr, the hyperfine structures and isotope shifts for the KrI n = 5,6,7 $4p^5ns$ Rydberg states were measured precisely with the VUV laser and (1 + 1) REMPI. Figure 3 is a typical trace of an isolated Kr transition, showing a laser-bandwidth limited resolution of 210 MHz. Using calibrated I_2 transitions as reference, the absolute position of each Kr transition can be determined to an accuracy of ± 0.01 cm^{-1}. This is a substantial improvement over existing values. By incorporating a time-of-flight mass spectrometer VUV transitions of each isotope (figure 4) and hyperfine spectra of ^{83}Kr (figure 5) were observed for the first time. Analysis of the results show that the $4p^56s$ and $4p^57s$ configurations of Kr can be described in a pure jj-coupling scheme as is normally assumed for inert gases, whereas the $4p^55s$ configuration shows a measurable departure from pure jj-coupling. All the ns configurations show some degree of mixing with the nearby $4p^5n'd$ configurations. It was also found in this series of experiments that contribution to the isotope shift is mainly from the mass effect, contribution from the nonzero volume is below the detectivity of the experiment.

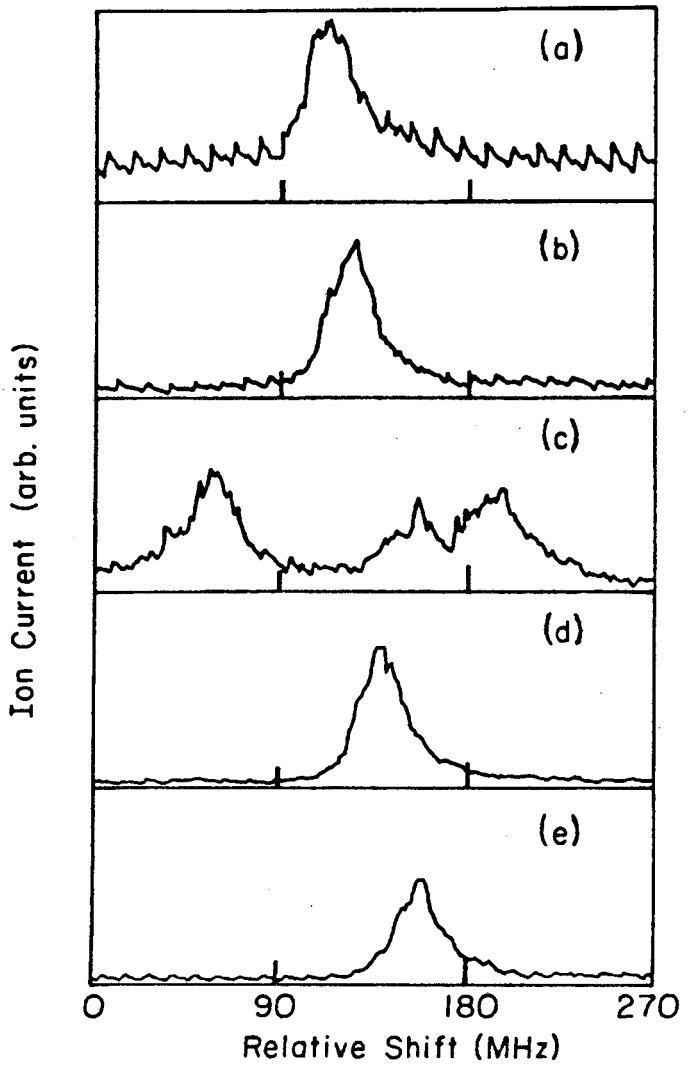

Figure 4. Relative isotope shifts for the 4p-7s $^2P_{3/2}$ (J = 1) transition of Kr for masses 80 (a), 82 (b), 83 (c), 84 (d) and 86 (e). Reprinted with permission from Reference 10.

Since two independent photons are involved in the (1 + 1) ionization process, it is possible to systematically delay the arrival of the second photon at the sample relative to the first one to probe the decay of the excited intermediate state. This was performed for the 6s and 7s states of Kr to obtain the lifetime of these states for the first time. The results are significantly different from theoretical predictions and should be useful as a basis for improvement of the theoretical results. These lifetimes and the results on Kr discussed above are tabulated in reference 10 and is not repeated here.

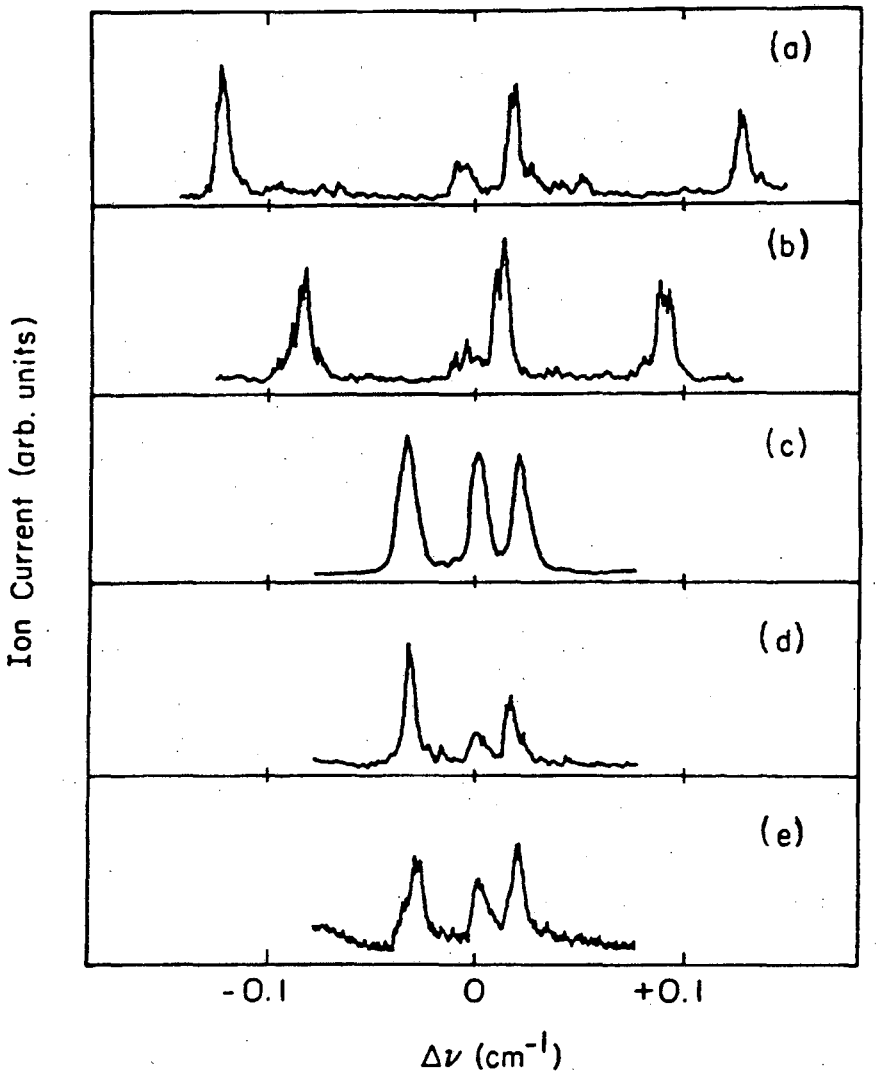

Figure 5. ^{83}Kr hyperfine structures observed for the 4p-5s' (a), -6s' (b), -5s (c), 6s (d) and 7s (e) $^2P_{3/2}$ $J=1$ transitions. Reprinted with permission from Reference 10.

IV. State-selective Ionization of Molecules

A large class of high resolution spectroscopic investigation that is made possible with (1+1) REMPI is the study of electronic states that are above the ionization threshold and are very weakly coupled to the ground state. Transitions involving such states include dipole-forbidden transitions and transitions with small Franck-Condon factors. In general, resonance with an intermediate level is not always necessary to access these states. However having the resonance not only substantially enhances the transition probability but also provides a high degree of quantum state selectivity to the excitation. Hence in contrast to the case of the previous section, the first photon in the process becomes a sample preparation step, the second photon is the one that does the investigation. Usually, then, the second photon is scanned

over a spectral region close to or above the ionization limit to search for high-lying Rydberg states and autoionization resonances. Alternatively the second photon excites the molecule to parts of its ionization continuum to render production of specific states of the ion. This final-state-selective ionization is the result of the $\Delta v=0$ propensity rule. Validity of this rule has been demonstrated in several cases.[13-17] This final state selectivity opens up many important possibilities. One such possibility is the production of vibrational-state-selective ions. It could facilitate studies of the chemical reactivity of excited state ions, a subject of tremendous current interest as demonstrated by articles by Baer and by Ng in this monograph. As an example, N_2 is used in our laboratory to illustrate the utility of the high-resolution VUV laser for state-selected ionization studies.[18]

N_2^+ is an important specie in atmospheric and stratospheric chemistry. There had been a number of attempts to produce state-selected N_2^+ using (n+1) REMPI where n is greater than 1. These approaches ran into tremendous complications because of the vicinity of a low lying N_2^+ A $^2\Pi_u$ electronic state to the N_2^+ X $^2\Sigma_g^+$ ground state.[19] Such complications can be minimized using (1+1) REMPI where the second laser is tuned close to the X $^2\Sigma_g^+$ $v^+ = 0$ and $v^+ = 1$ thresholds to avoid the A state. Figure 6 is a demonstration of this process. As laser 2 is tuned across the threshold for ionization to the ionic vibrational state, a new continuum is created. This signifies the production of ions in the corresponding vibrational state. In all cases the underlying continuum below threshold is practically zero. Hence very high selectivity is possible. In this experiment, several thousand ions were produced in a single pulse. With optimization this approach could produce large quantities of state-selected ions for experimentation. Many of the peaks in figure 6 have been identified to belong to new Rydberg states of N_2. These states cannot be reached from the ground state.

The experiment demonstrated that (1+1) REMPI is a versatile tool for studying spectroscopy in the 70 nm to 100 nm region of the spectrum. Extension of the technique to other diatomic molecules and triatomic and tetra-atomic molecules should be possible. The spectroscopy in this region is very rich, yet poorly understood, and dominated by highlying Rydberg states. For example, there is a variety of dynamical processes in direct competition in this high energy region: radiative decay, predissociation, autoionization, internal conversion, intersystem crossing, etc. Hence, work in this region of the electromagnetic spectrum should lead to many exciting new understanding of the chemical behavior of highly-excited molecules and atoms.

V. Molecular Reaction Dynamics

The ultimate goal in the microscopic investigation of unimolecular and bimolecular reactions is to be able to accurately describe how each reaction will proceed from initiation to completion. The most direct way to obtain this description is through theoretical scattering calculations when detailed information of potential energy surfaces is available. These calculations enable one to describe accurately how the parent molecular state is connected to the product state distribution in passing through the transition state. Significant progress has been made to having

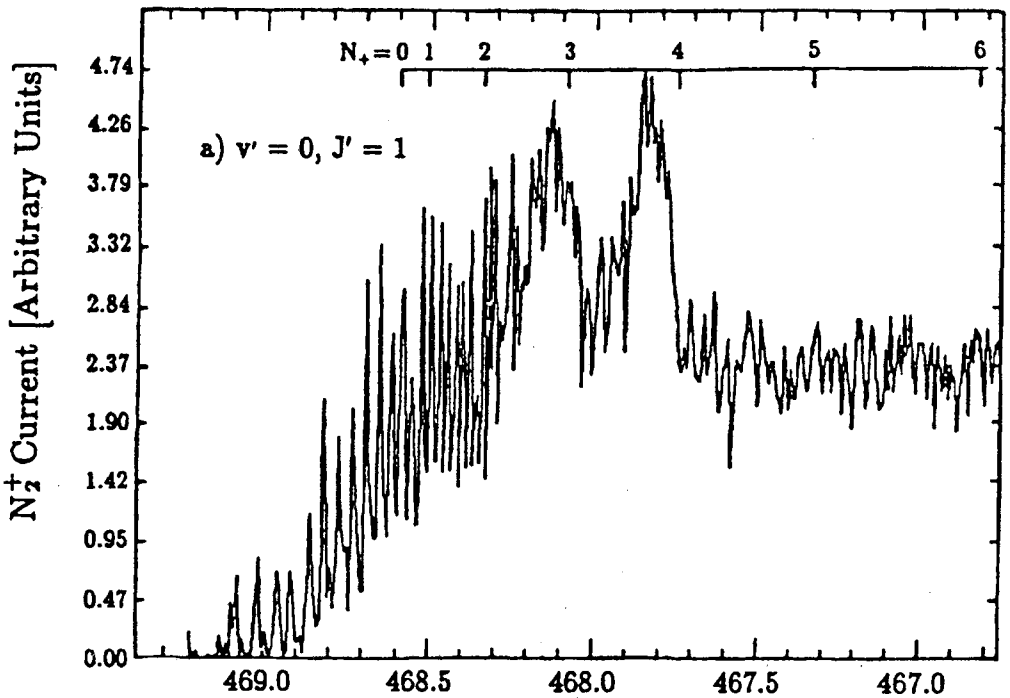

Figure 6. (1+1) photon ionization spectrum recorded with laser 1 tuned to the (0,0) R_0 line of the $c'_4 \leftarrow X$ transition of N_2. Bottom axis is wavelength of laser 2. Reprinted with permission from Refernce 18.

a full description of the simplest of all reactions: H + H_2 and D + H_2.[20-24] Here, agreement between theory and experiment is converging rapidly. However, for more complicated systems, for which either accurate potential energy surfaces are not readily available or scattering calculations are difficult, experimental probing of the nature of the potential energy surfaces often depend on the relation between initial conditions of reactants and final state distribution of products. In many H-atom transfer reactions, quantum mechanical dynamic resonances play an important role. The investigation of these resonances often provide detailed information around the transition state region of the potential surface. On the other hand, when a reaction possesses an exit potential barrier, especially in concerted decompositions eliminating a molecular specie, the final state distribution of products often reveal a clear picture of the structure and forces operating in the transition state region. There are in the literature excellent examples of using product energy distribution to elucidate the mechanism of photodissociation of simple molecules.[4-6,25,26] In this section we describe recent investigations in our laboratory of the elimination of H_2 molecule from 1,4 cyclohexadiene, and illustrate how one can elucidate the structure of the transition state region of this reaction by carefully measuring the vibrational, rotational, and translational energy distributions of the H_2 product using the (1+1) REMPI technique.[27]

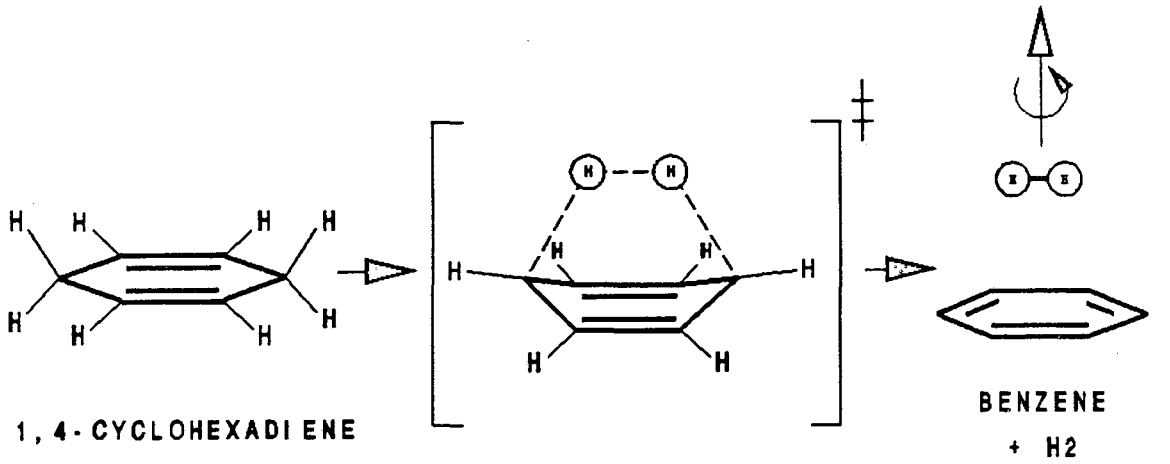

Figure 7. Pictorial description of the dynamics of photodissociation of 1,4 cyclohexadiene. Please see text for detail.

The dissociation dynamics of this reaction is of great interest because it is representative of a symmetric concerted H_2 elimination from a cyclic hydrocarbon. In a concerted dissociation, the potential energy surface along the reaction coordinate has an appreciable exit barrier due to the strained conformation of the reactant at the transition state. As is shown in figure 7, the structure of the transition state region will have a cyclic hexadiene in a boat form with two H atoms on 3,6 carbons approaching each other to facilitate the formation of the H_2 molecule. There are two coordinates which are important. The distance between the two H atoms, which is the vibration coordinate of the H_2 product, determines the final vibrational excitation in H_2. The other coordinate is the average distance between H_2 and the remaining benzene product. The repulsive interaction which depends on this average distance of the products determines the final translational energy distribution. For measurements of the vibrational, rotational, and translational energy distribution of H_2, the high-resolution VUV source is tuned through several H_2 transitions and the excited H_2 molecules are ionized by the accompanying UV radiation. A sample result of the experimental Doppler profiles for the H_2 C $^1\Pi_u \leftarrow$ X $^1\Sigma_g(2,0)$ P(9) transition and the C $^1\Pi_u \leftarrow$ X $^1\Sigma_g(2,0)$ Q(9) transition for the v=0, J=9 product state are shown in figure 8, along with the corresponding theoretical profile. Translational energy distributions are derived from iterative fitting of the experimental profile to the theoretical profile, which gives an average kinetic energy of $\approx$30 kcal/mole and a FWHM of $\approx$15 kcal/mole. This is in good agreement with measurements obtained by molecular-beam photofragmentation-translational spectroscopy.[28]

Product ro-vibrational state population can be derived from the integrated intensity of these profiles using accurately calculated oscillator strengths of the B$\leftarrow$X and C$\leftarrow$X transitions[29] and experimental parameters. What is found is that the rotational distribution in each vibrational level peaks at J"= 2 or 3, with the average J" decreasing slightly for the higher vibrations. A dominant fraction of the H_2 product appeared in v"=0 and not more than 20% had higher internal vibrational energies. The overall internal energy distributions can be characterized by a "rotational temperature" of $\approx$1600K and a "vibrational temperature" of $\approx$4000K.

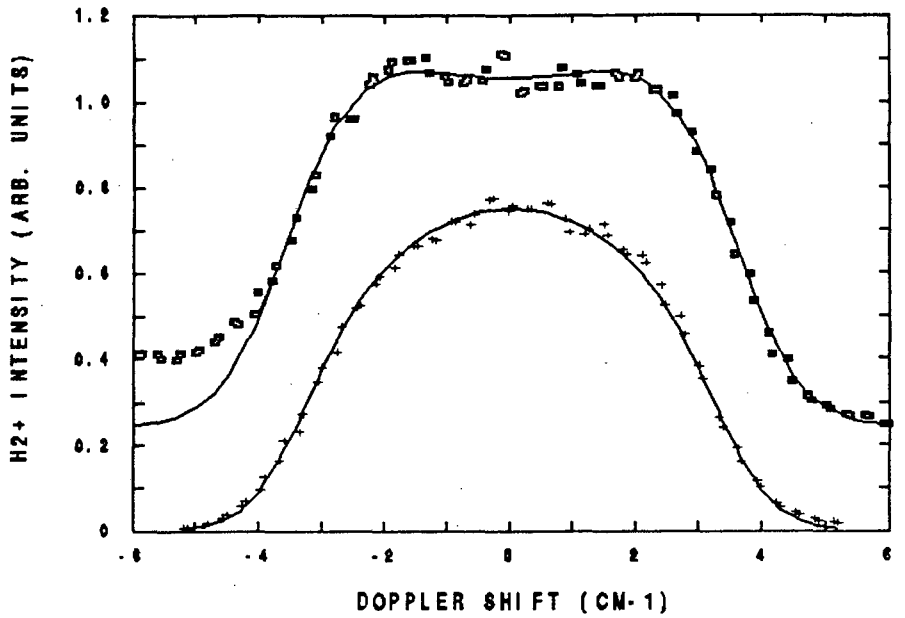

Figure 8. Doppler profiles of the product H_2 for the C $^1\Pi_2 \leftarrow$ X $^1\Sigma_g$ (2,0) P(9) transition (upper trace) and Q(9) transition (lower trace). Solid line is the corresponding least square theoretical fit.

These observations of low vibrational rotational excitation and high translational release point to a highly symmetric configuration for the transition state. The H's attached to the 3 and 6 carbons of the internally-excited cyclohexadiene move to a separation near the H_2 equilibrium distance while still strongly constrained by the original C-H bonds in the carbon ring just prior to release of the final product (figure 7). When the energy deposited in the molecule substantially exceeds the potential energy barrier, there is a wider range of structures near the transition state region that will lead to dissociation. At the same time, distortion from the highly symmetric structure of the parent molecule will cause asymmetry in the repulsive interaction and show correlation between the recoil velocity **v** and the angular momentum **J** of the H_2 fragment. This correlation can be deduced by careful analysis of the Doppler profile measured with a linearly polarized laser.[30,31] In the case of 1,4 cyclohexadiene, the results show a preferential alignment of **v** parallel to **J** just like a helicopter lifting off. Such an alignment was somewhat surprising given the number of degrees of freedom the parent molecule has to configure itself prior to dissociation. But it is clear that when two H atoms are pulled towards each other, bending motion of the C-H bonds which keeps the two H atoms in the plane of the benzene product is a lot easier to occur than the kind of motion which causes the C-H bonds to stretch or compress to keep H-H in the symmetry plane of the molecule which contains the 3,6 carbon atoms. The transition state structure for this latter motion would have caused the H_2 to fly off from the benzene like a frisbee rather than like a helicopter.

H_2 elimination is the primary pathway for an enormous number of molecular dissociation reactions. The cyclohexadiene experiment demonstrates that high-

resolution (1+1) REMPI is an extremely powerful tool for studying the mechanisms involved. For example, in the photofragmentation of ethylene eliminating H_2, it will be very interesting to probe the competition between a concerted three-centered elimination to form vinylidine and a concerted four-centered reaction to form acetylene. Detailed information concerning the structure in the transition state region of this reaction may be obtained by a complete product characterization using high-resolution (1+1) REMPI. Similarly, it is of fundamental as well practical interest to understand the primary dissociation dynamics of molecules like allene and other intermediate-sized hydrocarbons which are important species in combustion processes. Investigation along this line is underway in our laboratory.

VI. Future Possibilities

Ultrahigh resolution VUV lasers will undoubtedly play an extremely important role in future investigations of laser spectroscopy and laser chemistry. As more and more precise information on the electronically excited states are accumulated on various molecules and free-radicals, sensitive state-specific detection schemes of direct ionization or (1+1) REMPI will be applied in many experimental studies on the dynamics of chemical reactions and primary dissociation processes. Detection of N_2, CO, HF, HCl, HBr, F_2, Cl_2, as well as triatomic species like N_2O, CO_2, and HCN are obvious possibilities in the very near future. A great deal can be learned from experiments in which simultaneous determination of translational, rotational, and vibrational energies of molecules and the relation between the angular momentum vector and propagation vector are made. Having the ability to deliver photons in the narrowest possible spectral width will find widespread applications not only in high-resolution spectroscopy, but also in selective excitation of molecules, such as the case of sequential excitation, multiphoton excitation, and stimulated-emission pumping.

The dynamics of highly excited Rydberg states of medium-size molecules in other areas will benefit from the ultrahigh resolution VUV laser. There are many interesting questions concerning the competition among dissociation, autoionization, internal conversion, and intersystem crossing which are yet to be answered. Of course, these investigations will also lead to our better understanding of state preparation of medium-size molecular ions.

In spite of exciting prospects of the application of ultrahigh resolution VUV lasers in molecular science research, the high cost and the complexity of setting up and operating such a system will limit their availability at present. However, continuing developments in solid state, high power, high resolution tunable lasers, diode-pumped lasers, parametric oscillators, pulsed molecular beam techniques, and various oil-free pumping equipment will make it easier to construct a ultrahigh resolution laser, especially if reduced costs and significantly higher photon fluxes become a reality. A new revolution in laser spectroscopy and laser chemistry can be expected with ultrahigh resolution lasers leading the way.

VII. Acknowledgement

The authors wish to thank their colleagues, T. Trickl, E.F. Cromwell, M.J.J. Vrakking, D.J. Liu, A. Stolow, for their important contributions to the development and application of ultrahigh resolution VUV lasers described in this chapter. This work is supported by the Director, Office of Energy Research, Office of Basic Energy Sciences, Chemical Sciences Division of the U.S. Department of Energy under Contract No. DE-AC03-76SF00098 and the Air Force Astronautics Laboratory under Contract No. AFOSR F014611-87-K.

VIII. References

1. A.M. Wodtke and Y.T. Lee, in "Advances in Gas Phase Photochemistry and Kinetics, Vol I: Molecular Photodissociation Dynamics", M.N.R. Ashford and J.E. Baggott, Eds, Royal Society of Chemistry, London,1987,p.31.

2. D.H. Parker, in "Ultrasensitive Laser Techniques", D.S. Klieger, Editor, Academic Press, New York, 1983, and references therein.

3. A.H. Kung, T. Trickl, N.A. Gershenfeld, and Y.T. Lee, Chem. Phys. Lett. **144**, 427 (1988).

4. I. Burak, J.W. Hepburn, N. Sirckumar, G.E. Hall, G. Chawla, and P.L. Houston, J. Chem. Phys. **86**, 1258 (1987).

5. T.J. Butenhoff, K.L. Carleton, and C.B. Moore, **92**, 377 (1990).

6. L. Schnieder, W. Meier, K.H. Welge, M.N.R. Ashford, and C.M. Western, **92**, 7027 (1990).

7. P.R. Herman, P.E. LaRocque, and B.P. Stoicheff, **89**, 4535 (1988).

8. M.M. Salour, Opt. Commun. **22**, 202 (1977), and P. Drell and S. Chu, Opt. Commun. **28**, 343 (1979).

9. E. Cromwell, T. Trickl, Y.T. Lee and A.H. Kung, Rev. Sci. Instru. **60**, 2888 (1989).

10. T. Trickl, M.J.J. Vrakking, E. Cromwell, Y.T. Lee and A.H. Kung, Phys. Rev. **39A**, 2948 (1989).

11. D.A. Jackson, J. Opt. Soc. Am. **70**, 1139 (1980).

12. H. Gerhardt, et. al., Hyperfine Interactions **9**, 175 (1981).

13. S.R. Long, J.T. Meek and J.P. Reilly, J. Chem. Phys. **79**, 3206 (1983).

14. J.C. Miller and R.N. Compton, Chem. Phys. Lett. **93**, 453 (1982).

15. M.A. O'Halloran, S.T. Pratt, P.M. Dehmer and J.L. Dehmer, J. Chem. Phys. **87**, 3288 (1987).

16. S.T. Pratt, P.M. Dehmer and J.L. Dehmer, J. Chem. Phys. **80**, 1706 (1984).

17. W.E. Conaway, R.J.S. Morrison and R.N. Zare, Chem. Phys. Lett. **113**, 429 (1985).

18. T. Trickl, E.F. Cromwell, Y.T. Lee and A.H. Kung, J. Chem. Phys. **91**, 6006 (1989).

19. S.T. Pratt, P.M. Dehmer and J.L. Dehmer, J. Chem. Phys. **81**, 3444 (1984).

20. J.Z.H. Zhang and W.H. Miller, J. Chem. Phys. **91**, 1528 (1989).

21. D.L. Phillips, H.B. Levene, and J.J. Valentini, J. Chem. Phys. **90**, 1600 (1988).

22. R.E. Continetti, B.A. Balko, and Y.T. Lee, J. Chem. Phys. **93**, 5719 (1990).

23. D.A.V. Kliner and R.N. Zare, J.Chem. Phys. **92**, 2107 (1990).

24. S.A. Buntin, C.F. Giese, and W.R. Gentry, J. Chem. Phys. **87**, 1443 (1987).

25. Y. Chen, G. Hoffmann, D. Oh, and C. Wittig, Chem. Phys. Lett. **159**, 426 (1989).

26. M.P. Docker, A. Hodgson, and J.P. Simons, in "Advances in Gas Phase Photochemistry and Kinetics, Vol I: Molecular Photodissociation Dynamics", M.N.R. Ashford and J.E. Baggott, Eds, Royal Society of Chemistry, London, 1987, p.115.

27. E.F. Cromwell, D.J. Liu, M.J.J. Vrakking, A.H. Kung, and Y.T. Lee, J. Chem. Phys. **92**, 3230 (1990).

28. X. Zhao, R.E. Continetti, A Yokoyama, E.J. Hintsa, and Y.T. Lee, J. Chem. Phys. **91**, 4118 (1989).

29. E. Roueff, private communication.

30. P.L. Houston, J. Phys. Chem. **91**, 5388 (1987).

31. R.N. Dixon, J. Chem. Phys. **85**, 1866 (1986).

LAWRENCE BERKELEY LABORATORY
UNIVERSITY OF CALIFORNIA
INFORMATION RESOURCES DEPARTMENT
BERKELEY, CALIFORNIA 94720